CERN/DRDC 94-21
DRDC/P56
May 5, 1994

R & D Proposal

Development of Diamond Tracking Detectors for High Luminosity Experiments at the LHC

M.H. Nazaré
Universidade de Aveiro, 3800 Aveiro, Portugal

B. Foster, R.S. Gilmore, T.J. Llewellyn, R.J. Tapper
Bristol University, Bristol BS8 1TL, England

S. Roe, W. Trischuk*, P. Weilhammer
CERN, CH-1211 Geneva 23, Switzerland

P. Delpierre, A. Fallou, E. Grigoriev, G. Hallewell
CPPM, Marseille 13288, France

T. Ali, D. Barney, D.M. Binnie, P. Choi, J.F. Hassard, A.S. Howard, N. Konstantinidis, S. Margetides, J. Quenby, G. Rochester, R. Smith, T. Sumner, D.M. Websdale
Imperial College, London SW7 2BZ, England

L. Allers, A.T. Collins, V. Higgs, A. Mainwood
King's College, London WC2R 2LS, England

D. Kania, L. Pan
Lawrence Livermore National Laboratory, Livermore California, 94551, U.S.A.

P.F. Manfredi, V. Re, V. Speziali
Universita di Pavia, Dipartimento di Elettronica, 27100 Pavia, Italy
and
INFN – Sezione di Milano, 20133 Milano, Italy

C. Colledani, W. Dulinski, M. Schaeffer, R. Turchetta
LEPSI, Strasbourg 67037, France

S. Han, W. Kinnison, R. Wagner, H. Ziock
Los Alamos National Laboratory, Los Alamos New Mexico, 87545, U.S.A.

K.T. Knöpfle
Max-Planck-Institut Kernphysik, D69029 Heidelberg, Germany

D. Fujino, K.K. Gan, H. Kagan*, R. Kass, C. White, M. Zoeller
The Ohio State University, Columbus Ohio, 43210, U.S.A.

J. Conway, R. Plano, S. Schnetzer, S. Somalwar, R. Stone, R.J. Tesarek, G. Thomson
Rutgers University, Piscataway New Jersey, 08855-0849, U.S.A.

R. Frühwirth, J. Hrubec, M. Krammer, G. Leder, H. Pernegger, M. Pernicka
Institut für Hochenergiephysik, Österr. Akademie d. Wissenschaften, A-1050 Vienna, Austria

* Spokespersons.

Abstract

The LHC offers unique physics opportunities in an extremely difficult operating environment. Diamond is a material with such extraordinary physical properties – many of which address the problematic LHC operating conditions – that we wish to explore its use in a variety of ways.

Tracking detectors have become an important ingredient in high energy physics experiments. In order to survive the harsh detection environment of the LHC, trackers need to have special properties. They must be radiation hard, provide fast collection of charge, be as thin as possible and remove heat from readout electronics. The unique properties of diamond allow it to fulfill these requirements. Further, recent progress in the production of chemical vapor deposited diamond makes large surface area detectors now realistic. We propose a development program which improves the charge collection properties of diamond, studies the radiation hardness of the material, designs various tracking devices, develops low noise, radiation hard electronics to read out the detectors and applies diamond as a thermal management tool for the LHC.

Our proposal combines the forces of universities and (inter)national laboratories, as well as researchers from disciplines not traditionally associated with high energy physics. We have assembled a team with the capabilities of solving the remaining issues in the development of diamond as a particle detector. If we succeed, it will be possible to operate tracking detectors in the highest radiation areas of the LHC.

Contents

1 Physics Using Diamond Detectors

Two of the outstanding problems in high energy physics today are the generation of mass through electroweak symmetry breaking, the Higgs mechanism, and a better understanding of quark mixing, the study of CP violation. The primary goal for the LHC is to address these questions. The study of these physics issues will not be easy; it requires the highest available beam energy and the highest possible luminosity. This means that the events will have to be extracted from complex backgrounds. Our goal is to develop a tracking detector that we can deploy extremely close to the interaction point which will allow us to extract these important signals from the background.

1.1 LHC and Diamond Characteristics

The LHC will operate at $\sqrt{s}$=15.8 TeV and luminosities which start at a few times 10^{32} cm^{-2} s^{-1} and increase to 10^{34}cm^{-2} s^{-1} over several years. These luminosities will enable us to explore the physics issues posed above. Under the LHC experimental conditions the average charged multiplicity is over 300; at high luminosities up to fifty *pp* interactions per bunch crossing - every 25ns - will occur; the radiation levels 10 cm from the beam amount to 2 x 10^{13} neutrons cm^{-2} year^{-1}. Clearly, in the inner regions of the central detectors, ATLAS[1] and CMS[2], pattern recognition, radiation hardness and thermal management are major issues. In the proposed dedicated *b* experiments, COBEX[3], GAJET[4] and LHB[5], very difficult environments and demanding event topologies must also be overcome.

Two approaches have been taken to solve these problems. One is to modify existing detector technologies to adapt them to the task at hand – silicon is a clear example [6]. Another approach is to take a material which has the inherent properties required to survive at the LHC and use it to develop detectors. Our group proposes to take the second approach; the material we have chosen is diamond. The properties of diamond which attract us to this approach are:

- Diamond is radiation hard, essential in the environment of the LHC;
- Diamond is an excellent insulator with a high breakdown voltage, allowing the application of a large electric field to attain a saturated drift velocity while maintaining a very low leakage current;
- Diamond is extremely fast to read out. We can collect all of the charge within 1ns [7, 8] - diamond may be the only material in which the charge can be collected much faster than the machine repetition rate;
- Diamond has low Z. This ensures that the multiple scattering, δ-ray production[9] and photon conversion rate in diamond will be small. The implications in vertex finding are obvious, particularly in the fixed target and forward collider configurations;
- Diamond has a smaller dielectric constant than silicon. The components of detector noise which depend on the dielectric properties of the material will be minimised;

- Diamond is the best known thermal conductor at normal temperatures, and has the one of the lowest known coefficients of thermal expansion;
- Diamond is physically robust. It does not need a supporting substrate like glass. Again, this allows us to minimise multiple scattering;
- Diamond requires processing which is relatively simple. Its present total cost is similar to that of silicon, however, unlike silicon this cost is mainly in the initial production, whose prices have declined greatly, and continue to fall sharply.

In the general purpose detectors, CMS and ATLAS, we identify two possible roles for diamond tracking layers: in the central region, where it is possible to position planes very close to the beampipe, and outside the central region where it is desirable to tag the decay vertices of B mesons. In the current proposals for CMS and ATLAS such tagging is not fully optimised.

As a further example, consider the dedicated beauty experiments proposed for the LHC. High precision vertex detectors are necessary to reconstruct vertices in forward-boosted jets containing around 60 charged tracks. In the LHB experiment the "forward" nature of the tracks, coupled with the enormous flux of beam particles which do not interact in the target, means that severe radiation damage will occur in local regions of the forward detectors; the LHB collaboration has proposed moving the complete vertex detector system transverse to the beam direction, by some tens of microns, every few minutes in order to spread the radiation dose more uniformly. The miniscule signal to background ratios at all dedicated beauty hadroproduction experiments means that complex triggers must be used; placing detectors close to the interaction region extends the efficiency of both topology triggers (especially at high luminosities) and muon triggers. In COBEX, a 600 mrad aperture may be necessary in order to reduce radiation levels in the very forward region and, as with GAJET, this means that vertex detectors must be inserted into the beam pipe in Roman pots. If these detectors were made of silicon they would need to be replaced on a regular basis.

1.2 LHC Radiation Levels

Radiation levels expected at the LHC have been derived from computer codes[10] and extrapolations from experiments. There is necessarily some uncertainty associated with both methods. Additional uncertainty comes from the beam-dependent production of neutrons, for example in ATLAS and CMS, coming from elements of forward calorimetry and collimators activated by particles from the primary interaction.

The numbers given here refer to years of 10^7 seconds at $\mathcal{L} = 10^{34}$ cm^{-2} s^{-1} unless otherwise specified. The radiation dose can be divided into that due to electromagnetic interactions (primarily from photons, but with significant charged particle contributions), and from neutrons. Neutron fluxes quoted are for particles more energetic than 100 keV, below which energy silicon appears to be immune to damage. The threshold for diamond is not accurately known, but is expected to be significantly higher.

In ATLAS and CMS the neutron flux is quoted as being isotropic due to the albedo from the thick calorimeters at a value of 3×10^{12} n cm^{-2} year^{-1} of average energy 1 MeV[11]. However, detailed studies[12, 13] have shown that there is weak z dependence and a radial dependence of $1/r^2$ from the primary vertex imposed on the albedo neutron flux. This results in a rate of approximately $0.8 - 2.0 \times 10^{13}$ n cm^{-2} year^{-1} at $z = 0$, $r = 10$ cm rising to 2.5×10^{13} n cm^{-2} year^{-1} at z=300cm.

The electromagnetic flux is expected to be simpler in form, falling as $1/r^2$. It could total as much as 0.1 MGy per year 6 cm from the interaction point in ATLAS and CMS.

In both the fixed target and forward collider b experiments, the neutron flux is expected to originate from the primary interactions, and is likely to be only a minor problem. The radiation dosage can be estimated from the expected flux:

$$\Phi = \frac{N_{beam}}{S}\left(1 + \frac{L_T}{\lambda_I}\langle n_{ch}\rangle\right) \text{[5]}$$

where N_{beam} is the integrated beam flux, $\frac{L_T}{\lambda_I}$ is the target thickness in interaction lengths and $\langle n_{ch}\rangle$ is about 60 in LHB, as mentioned above. The absorbed dose D in Gy, in the silicon vertex detector is then D = $2.6 \times 10^{-16} \times \Phi$ amounting to about 0.1 MGy per year. Similar considerations apply to COBEX and GAJET.

This problem affects experiments in other colliders as well. In the HERA-B proposal[14] a flux of $\Phi = 3 \times 10^{14}$ particles (mainly pions) cm^{-2} year^{-1} is expected at $r = 1$ cm. Relatively few neutrons - of order 15% as expected. Again, regular replacements of the vertex detector are planned and diamond is considered to be an interesting option[14]. As is shown (later) preliminary results indicate diamond's ability to withstand these rates.

Given the extreme radiation level close to the interaction point, diamond based detectors may well be the only solution for vertex tracking devices.

1.3 Vertexing and Track Finding

Vertexing and the use of impact parameter information have long been recognised as powerful methods for isolating charm and beauty particles. Recent studies at LEP of , $_{b\bar{b}}$ rely heavily on silicon vertex detectors to efficiently separate b final states from other final states of Z^0 decay. We expect the same techniques will play a critical role at the LHC.

The impact parameter precision in the central regions of collider detectors like ATLAS and CMS, is given by: $\sigma_{ip} = (A^2 + (B/P_T)^2)^{1/2}$ where A is heavily dependent on layer positioning and hit precision. B depends on the distribution of material. In this formula P_T is in GeV/c and σ_{ip} is in microns. Both parameters are reduced if detectors are made of low Z material and are placed at small radii. In ATLAS these parameters are currently about 30 μm and 220 μm respectively[15]. With a 6 cm radius detector, they would be reduced to 14 μm and 72 μm respectively.

Figure 1 shows how the precision of the impact parameter measurement varies as a function of the radius of the first tracking layer in ATLAS. Similar plots exist for CMS. These plots show that the impact parameter resolution is halved for high

Signal	Background	Reference	Comments
$H^0 \to ZZ \to l^+l^-l^+l^-$	$t\bar{t} \to l^+l^-l^+l^-$, $Zb\bar{b} \to l^+l^-l^+l^-$, $ZZ^* \to l^+l^-l^+l^-$	[20],[21]	$\sigma_{ip} \leq 50\mu$m for b discrimination
H $\to WW \to l\nu jj$, H $\to ZZ \to l\bar{l}$jj	$QCD \to l\nu$jj	[22]	$\sigma_{ip} \leq 50\mu$m for b discrimination
t$\to H^{\pm}b$,$H^{\pm} \to \tau\nu$, $H^{\pm} \to$cs	$b\bar{b}$, $W + jet$, $t \to W \to \tau$	[1] [23],[24]	$\sigma_{ip} \leq 50\mu$m for b discrimination
$H^0, A^0 \to \tau\tau$			
$t\bar{t} \to W(\to \mu\nu)$ $+W^- + b/\bar{b}(\to \mu)$ $t\bar{t} \to W(\to \mu\nu) + W^-$ $+$b$/\bar{b}(J\vert\psi) + b/\bar{b}(\to \mu)$	$b\bar{b}$	[19],[22] [25]	$\sigma_{ip} \leq 50\mu$m $t \to$jjb gets $\delta(m_t) \sim$0.1 GeV
$B_d \to J\vert\psi K^*$	combinatorics		control channel for $B \to J\vert\psi K_s^o (ie\ \beta)$
$B_d \to \pi\pi$	combinatorics	[26]	α
$B_s \to \rho K^o$	combinatorics	[26]	γ
$B^{**\pm} \to B^0\pi^{\pm}$ $\to (CP\ eigenstate)\pi^{\pm}$	combinatorics	[27]	Intrinsic tagging
Pb + Pb$\to J\vert\psi, \Upsilon$	2300 tracks per unit η	[28]	eg $\sigma = 20\mu$m in vertex separates Υ' from Υ''

Table 1: Physics channels which benefit from more precise tracking.

momentum tracks, typical of a new particle searches at the LHC, while it is reduced by almost a factor of three for low P_T tracks, typical of B decays. The detector capabilities are greatly enhanced by the addition of a tracking layer within 6 cm of the interaction point. Diamond is one of the few materials with the properties to survive in this region.

Small detector radii and large minimum bias backgrounds (and in CMS, a large magnetic field) make track-hit assignments difficult. Given the channel density, correct assignments are manageable provided alignment can be achieved to better than $\simeq 10\mu$m [16]. Using a signal to noise ratio of approximately 15 to 1, we find better than 97% correct track-hit assignment, acceptable in most physics cases.

1.4 Possible Roles for Diamond in LHC Physics

The ATLAS and CMS collaborations have concentrated upon the central region – a reflection of the kinematics of main LHC goals: the Higgs[17], supersymmetry[18] and the top quark[19]. In table 1, we list the channels in which diamond detectors could play a leading role.

The production of B mesons in colliding beams is fairly uniform in pseudorapidity out to $\eta = \pm 2.5$, so the regions with $\mid \eta \mid \geq 1$ assume greater importance. This is outside the acceptance of central cylindrical trackers. A set of forward trackers is necessary. It can be shown that the optimal configuration for these detectors is to

Inner layer radius	Z Vertex Precision
6cm	46.5μm
8cm	48μm
10cm	52.5μm
18cm	78μm

Table 2: Isolating the Event Vertex in CMS

place them normal to the tracks and space them equidistant in the logarithm of z, the distance from the interaction point along the beampipe[16]. A figure of merit here is the accuracy with which we resolve the decay length of a B. For example, in the process, $B \to J|\psi K_s^o, J|\psi \to \mu\mu$ we must reconstruct the $J|\psi$ vertex by extrapolating the two muons to their production point. Since the average boost of the B increases at higher rapidities we get a vertex precision significance, S, of greater than 3 out to $\eta = 2.25$, where S $= \frac{(\gamma\beta c\tau)_B}{\delta(\gamma\beta c\tau)_B}$. This is useful in background reduction, tagging and even the measurement of the CP asymmetry time variation out to rapidities of 1.3. This is shown in fig. 2.

1.5 High Luminosities

Almost all physics goals requiring particle-particle or particle-vertex correlations in high luminosity LHC running will require vertex discrimination. At the highest luminosities, we expect up to 50 interactions per crossing. They will have mean nearest-neighbour separation in the z view, of about 1.5 mm. With a vertex precision of a few hundred microns, the efficiency of finding vertices becomes important in separating neighboring interactions. The benefit of inner vertexing layers is shown in table 2. This comes from a simulation of the CMS detector, in which conventional geometries and resolutions have been augmented by the addition of an extra barrel layer of diamond with hit precisions of 15 microns.

1.6 Summary

The possibility of extending detector reach to smaller radii and greater rapidities offers new physics potential for the LHC. Given the hostile physical conditions near the interaction regions, detector material with extraordinary properties is required. Diamond's physical hardness, electronic speed, radiation hardness, thermal properties and favorable radiation length, make it an intriguing option for this specialized niche at the LHC.

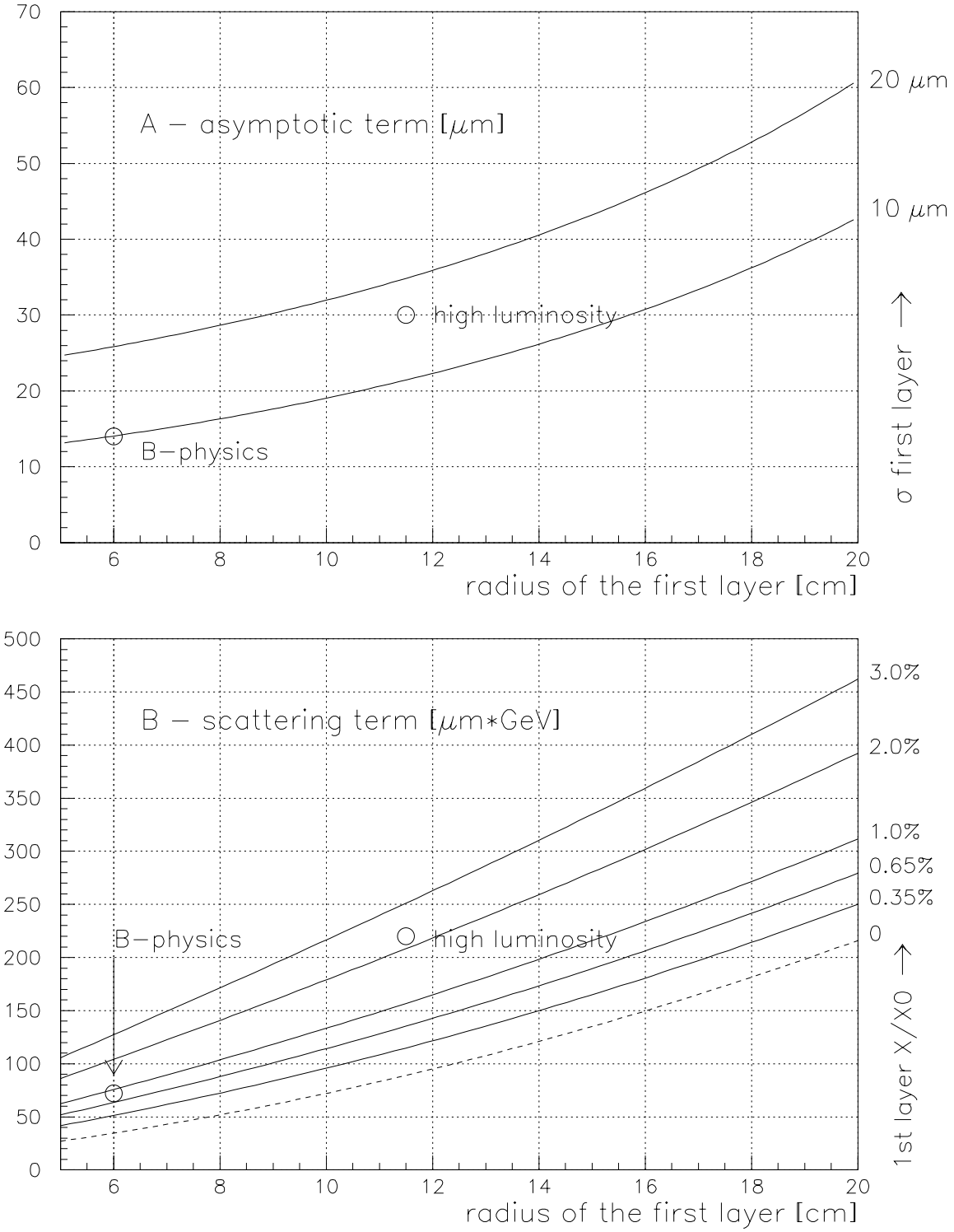

Figure 1: The top plot shows the change in A (see text) as a function of the radius of the inner layer of tracking for two different hit precisions (10 μm and 20 μm). The bottom plot shows the change in B as function of the radius for several detector thicknesses. The "high luminosity" point is the current configuration of ATLAS, while the "B–physics" point could be realised with a sufficiently radiation hard tracker.

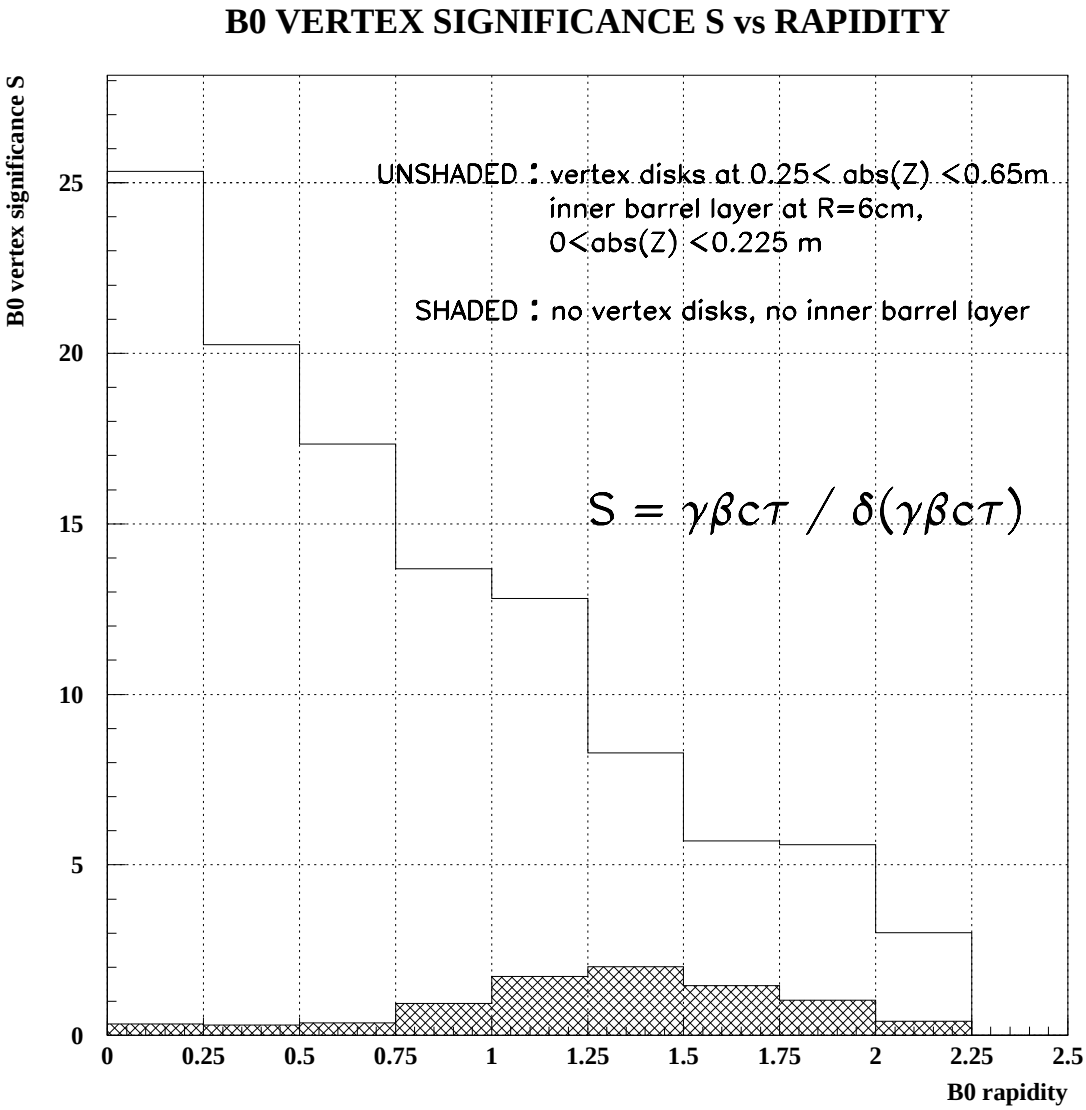

Figure 2: The B vertex reconstruction significance. With the addition of a diamond vertexing layer and a set of forward disks the CMS tracker is able to reconstruct B decay vertices with greater than three sigma accuracy out to $\eta = 2.2$ (unshaded histogram). Without these additional tracking layers, the significance of a B decay vertex measurement does not exceed three sigma for any η (shaded histogram).

2 Diamond as a Detector Material

In figure 3 we show the basic principle of the use of diamond as a charged particle detector. A DC voltage of a few hundred volts is applied across a layer of diamond a few hundred microns thick. When a charged particle traverses the diamond, atoms in the crystal lattice sites are ionized, promoting electrons into the conduction band and leaving holes in the valence band. On average, approximately 3600 electron hole pairs are created per 100 μm of diamond traversed. These charges drift across the diamond in response to the applied electric field producing a signal that can be amplified and processed.

2.1 Properties of Diamond

In table 3 [32] we summarize the properties of diamond (and for comparison silicon) that are of interest when considering this material for use as a particle detector. Since diamond has a large band gap, 5.5 eV, it is a very good electrical insulator. The conductivity of actual diamond material is, in fact, dominated by the presence of defects and impurities. Nevertheless, the resistivity of high-purity natural IIa diamond is typically 10^{12} Ω-cm to 10^{16} Ω-cm. Because of this large resistivity, a high electric field can be applied across the diamond layer without producing significant leakage current. Thus there is no need, as in the case with silicon, for reversed biased pn-junction to prevent large leakage currents whose fluctuations would dominate the signal.

Compared with silicon the electron mobility is slightly higher in diamond while the hole mobility in diamond is two times larger and is approximately equal to its electron mobility. More important, the larger $E_{breakdown}$ of diamond means these detectors can be operated at the saturation velocity. Thus in a diamond detector with thickness of a few hundred microns, the charge collection time is about 1 ns.

Although diamond is an electrical insulator it is also an excellent thermal conductor. At room temperatures, the thermal conductivity of diamond exceeds copper by about a factor of five. A common problem with large strip detector systems is the management of the thermal load generated by the large number of electronic channels used in the detector readout. The handling of this thermal load will be greatly simplified if the detectors or even the substrates used for the detector electronics are constructed from diamond.

Diamond has two additional properties which may play an important role certain applications. Its small dielectric constant means that the components of capacitance in detector configurations which depend on the dielectric properties of the material will be minimized. In addition, since diamond detectors do not require diodic structures, this material is immune to many of the plagues of high radiation environments including type inversion.

Diamond material appears ideal in many applications but it does have limitations: the large band gap which determines many of its outstanding properties also means that its signal size is not large, *i.e.* approximately half that of silicon. This effect may be compensated for, in certain configurations, by its smaller dielectric constant

Property	Diamond	Silicon
Band Gap [eV]	5.5	1.12
Breakdown field [V/cm]	10^7	3×10^5
Resistivity [Ω-cm]	$> 10^{11}$	2.3×10^5
Intrinsic Carrier Density [cm^{-3}]	$< 10^3$	1.5×10^{10}
Electron Mobility [$cm^2V^{-1}s^{-1}$]	1800	1350
Hole Mobility [$cm^2V^{-1}s^{-1}$]	1200	480
Saturation Velocity [km/s]	220	82
Dielectric Constant	5.7	11.9
Cohesive Energy [eV/atom]	7.37	4.63
Thermal Expansion Coefficient [K^{-1}]	0.8×10^{-6}	2.6×10^{-6}
Thermal Conductivity [W m^{-1} K^{-1}]	1000-2000	150
Energy to create e-h pair [eV]	13	3.6
Mass Density [gm cm^{-3}]	3.5	2.33
Ave Number of e-h Pairs Created/100 μm [e]	3600	9200
Ave Number of e-h Pairs Created/0.1% X_0[e]	4500	8900

Table 3: The physical properties of diamond and silicon at 293K.

and hence smaller capacitance.

2.2 Chemical Vapor Deposition Diamond

The research effort described in this document makes use of artificial diamond manufactured using the Chemical Vapor Deposition (CVD) process [30]. In the CVD process, a hydrocarbon gas, such as methane, is mixed with a large concentration of molecular hydrogen gas. The gas mixture is then excited by either microwaves, a hot filament, or some other energy source. The resulting reactive gas mixture is brought into contact with a substrate, typically silicon, where the carbon based radicals are reduced and link together with single bonds (sp^3 hybridized orbitals) forming a diamond lattice. A large concentration of atomic hydrogen is a crucial part of the process and is believed to play two separate roles in promoting diamond growth. It hydrogenates the surface of the film thus preventing the formation of graphitic bonds, and also serves to etch any graphite that happens to form since hydrogen reacts much more readily with graphite than with diamond. Raman spectroscopy and X-ray diffraction have unambiguously shown that the CVD grown films are diamond and polycrystalline in structure.

CVD diamond typically grows in a polycrystalline columnar structure along the growth direction. The substrate side begins with small grains ($\sim 1\mu$m) which grow with material thickness. As the material grows it develops the texture of the fastest growing crystal orientation. The CVD diamond has a random orientation on the substrate and a (110) texture on the growth side. It has recently been shown [31, 33, 32] that the electrical properties of CVD diamond vary with the thickness of the material; the carrier lifetime and mobility are small on the substrate side and large on the growth side. As a result, the raw CVD diamond material can be "improved" by removing material from the substrate side. This procedure has been used and has

increased the collection distance by 40% over the as-grown sample.

The CVD growth of diamond can be achieved through several processes and many companies * and universities in Europe, Japan and the US are producing polycrystalline CVD diamond films. Nevertheless, this is still a developing field and there are a large number of parameters which must be optimized for the production of the quality diamond necessary for charged particle detectors. These include: type of excitation energy source, relative concentration of hydrocarbons, substrate temperature, gas pressure, etc. Different parameters lead to different properties of the resulting diamond. Because of the large number of variables, systematic correlations between growth parameters and film quality are only now being developed.

2.3 Recent Progress

The CVD process shows promise of solving the major problems limiting the traditional use of diamond: the high cost and the large trapping center density which leads to a short carrier lifetime, and charge buildup. In contrast to the more familiar high-pressure, high-temperature diamond synthesis methods, which produce crystals typically 1 mm in size, CVD production has been scaled efficiently to cover large areas on 18 cm diameter wafers. Out of such wafers, detectors have been fabricated [34]. This opens the possibility of single large area detectors. In addition, the CVD process allows the formation of non-planar detectors to fit the needs of the experiment.

A major part of this proposal involves the development of higher quality CVD diamond. In order to attain this goal we have developed a set of characterisation procedures (see below) to classify diamonds. Foremost among these is a measurement of *collection distance*, the average distance an electron and hole, created by the passage of an ionizing particle, move apart under the influence of an applied electric field. This quantity is directly related to the detection capabilities of the diamond. In fig. 4 we show the measured collection distance as a function of year. Since we have begun our development program the quality of CVD diamonds has increased by nearly three orders of magnitude. Moreover, recent work by members of our group indicates that there are still large gains to be made in the coming years.

Recently the unique properties of diamond have allowed it to be used where other materials have failed. The first application involves the measurement of ionizing radiation in the presence of a large low energy photon background. The 5.5 eV band gap allows a diamond to detect charged particles in a severe photon background since diamond is transparent to photons ie. blind, with sub-bandgap energies ($\lambda > 220$ nm). The second application involves work recently de-classified by the U.S. government where the high radiation resistance of diamond allowed it to be used to understand thermonuclear reactions and laser induced fusion.

*We are in contact with the following CVD diamond manufacturers: AEA Technology, Crystallume, de Beers, Kobe Steel and St.Gobain/Norton.

Figure 3: Schematic view of a diamond detector.

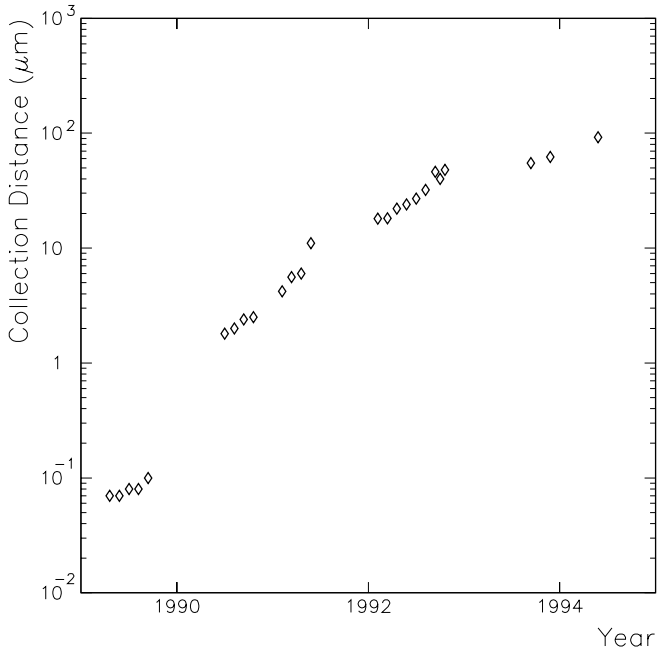

Figure 4: The recent history of collection distance of CVD diamond.

3 Radiation Damage in Diamond

High energy particles displace atoms in the diamond lattice to produce vacancies and interstitials. It is known that 2 MeV electron irradiation produces about 0.3 neutral or negatively charged vacancies per electron cm^{-1}[35, 36, 37], and these can be recognised by their optical spectra. The vacancies are immobile below about 650°C[36]. A similar number of interstitial atoms are also produced and these may be mobile at much lower temperatures (electron spin resonance data indicate 50K[38]). The interstitials can be detected optically in certain trapped states[39]. Although it is not known how these primary defects affect the electronic properties of the diamond[40]; scattering by charged defects has been shown to be an important mechanism which limits the collection distance of CVD diamond[41].

In silicon, similar damage produces about ten times as many primary defects[42], which are mobile at very low temperatures. About 90% of these defects recombine leaving net damage about the same as in diamond. However, the mobile defects form complexes which are electrically active, and affect the detection efficiency of the silicon device.

Damage of diamond by electrons has been thoroughly investigated [43]. Early data [44] indicate that neutrons produce about 500 times the number of vacancies as those produced by electrons. This constitutes a considerable concentration of primary defects under the conditions that the detectors will undergo. It appears that these primary defects have very little effect on the electronic properties of the detectors [45]–far less so than for silicon [43]. However, if diamond detectors are to be used in regions of very high radiation, the effects of radiation damage must be investigated in more detail. We need to understand the details of the damage and its effects on the electronic properties of the diamond so that detectors can be designed to minimise the loss of performance as a result of damage.

There are two primary manifestations of radiation damage in solid state detectors. One is an increase in leakage current and the other is a decrease in pulse height. The tightly bound lattice structure of diamond suggest that it will be insensitive to large doses of radiation. Studies[46, 47] have shown that diamond detectors are very resistant to both types of damage.

The increase in leakage current, in silicon detectors for example, arises from radiation-induced defects that produce states with energies that are within the band gap. These sites act as current generation centers emitting electrons into the conduction band and holes into the valence band which are immediately swept out of the depletion region by the applied field. Since, in the depletion region, the carrier concentration is not in equilibrium, the generation current is proportional to the intrinsic carrier concentration[48]. Since no *pn*-junction is required in a diamond detector, there is no depletion region and the carrier concentrations are in equilibrium. The recombination rate is, therefore, equal to the generation rate and there is no net generation/recombination current. As a result, the amount of radiation induced leakage current is negligible for diamond detectors.

The other effect of radiation damage is a decrease in the observed pulse height. This is due to the production of trapping centers which results in a decrease in carrier lifetime. These trapping centers can be produced by charged particles or neutrons

causing lattice defects. Diamond with its large cohesive energy and tight lattice structure is also resistant to this type of damage.

Ion implantation studies of diamond have shown that even very severely damaged samples can be at least partially restored by annealing at 1450K[49, 50]. At these temperatures the vacancies are extremely mobile, and it is assumed that they either recombine with interstitials, or migrate to distant traps leaving a relatively undamaged lattice.

3.1 Current Studies of Radiation Damage in CVD Diamond

During the last few years we have undertaken several studies of radiation damage to CVD diamond detectors. These were tests which were designed primarily to look for evidence of radiation damage rather than to understand the underlying damage mechanism. One study measured the effects of a large fluence of low energy alpha particles. Another looked for damage due to low energy gamma irradiation. Future work will concentrate on neutron and charged pion damage.

3.1.1 Low Energy Alpha Irradiation

Two years ago, we initiated a study of diamond detector damage due to an intense beam of 5 MeV alpha particles. These particles have a penetration depth in diamond of only about 12 μm. A surface photo-induced conductivity measurement of the collection distance at the beam focus was made before and after successively larger doses.

Figure 5 shows the results after 4 dose levels, both in terms of fluence and deposited energy. At a fluence of $2\text{x}10^{13}$ alphas cm^{-2} the collection distance was reduced to about 80% of the unirradiated value. At $2\text{x}10^{15}$ alphas cm^{-2} the collection distance was reduced to 40% of the unirradiated value. This exposure corresponds to approximately 50 MGy which is much larger than the expected lifetime dose at the LHC.

3.1.2 Low Energy Photon Irradiation

We have recently completed a study started in 1993, using a ^{60}Co gamma (1.2 and 1.3 MeV) source at Argonne National Laboratory. Bulk collection distance measurements were made before and after each irradiation. As can be seen in fig. 6, up to and including a 0.1 MGy dose, there is *no evidence* of degradation of electronic properties in CVD diamond.

An interesting effect was observed at low dose (less than 0.1 kGy) levels: the collection distance improves with accumulated dose. This effect is not understood but may be due to the eventual passivation of charge traps by charge carriers created by the ionizing radiation.

3.2 Future Radiation Damage Studies

In the next few months we will establish a program of neutron irradiation. For

each irradiation, we will include a type IIa natural diamond, a silicon photodiode, as well as CVD diamond samples. This will allow for direct comparisons of signal loss among these materials at every dose level.

During the DRDC proposal period, we plan to expose samples of the newest CVD diamond material to neutron, alpha and ^{60}Co sources as new generations of the material become available. We also expect to establish a study of irradiation with charged pions and protons.

We also propose to investigate quantitatively the production of specific defects (vacancies, interstitials and their complexes), by irradiation, to see which defects affect the electronic properties, and by how much. We will compare the results under irradiation by different particles, at a range of energies. This will allow us to identify any impurities in the diamond which might exacerbate or passivate the consequences of the damage. From these studies we expect to demonstrate whether variations in the production process affect radiation hardness and to work to optimise the growth of radiation-hard diamond.

In addition, annealing studies of the irradiated diamonds will show if the electronic properties of a detector, degraded by high radiation dose and can be improved by heat treatment.

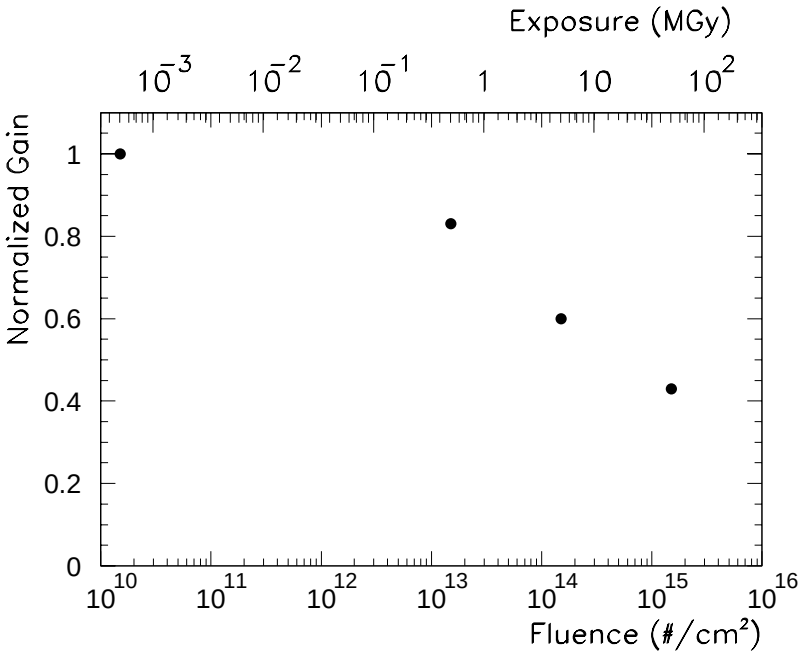

Figure 5: Exposure of CVD diamond to 5 MeV alpha particles. Normalized gain (compared to the unirradiated gain) as a function of increased fluence. Top scale is exposure in MGy.

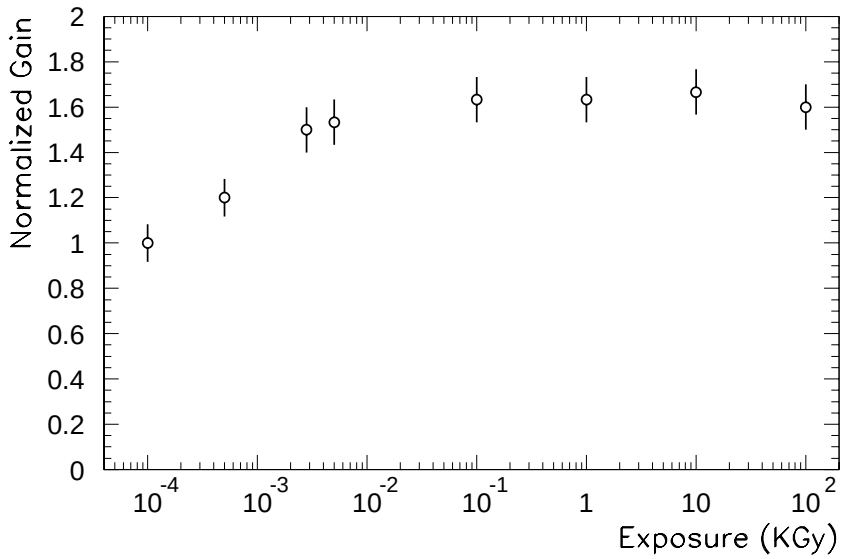

Figure 6: Exposure of CVD diamonds to ^{90}Sr and ^{60}Co photons. The first four points were Sr irradiations while the others were done with Co.

4 Diamond Strip Trackers

High precision strip detectors are an important tool for the study of long lived particles in present high energy physics experiments and are an integral part of the initial configurations of LHC detectors. At the highest luminosities both the ATLAS and CMS experiments are planning to replace the inner layers of silicon on a regular basis. Clearly one area which deserves attention is the development of detector technologies which are capable of withstanding the high rates and particularly severe environments of the LHC. One aim of our three year program is to demonstrate CVD diamond strip detectors yielding on average ≥ 7000 e's signal from 300 μm of material which can tolerate the expected radiation levels. This represents an increase in the quality of presently available CVD diamond by approximately a factor of four.

4.1 Principles of Operation

The basic parameters which allow diamond to perform in the hostile environment of future colliders are shown in table 3 [29]. For the purposes of constructing high precision, radiation hard strip detectors, the parameters of interest are the large band gap and low intrinsic carrier density which imply low leakage currents, the large resistivity which implies that ohmic contacts may be used to sense the charge created during ionization, the large breakdown voltage which implies stable operation, and the large cohesive energy which implies good radiation resistance.

In fig. 7 we show a schematic view of a single sided diamond strip detector. The basic detector consists of $\sim 300\mu$m thick wafer of diamond, a series of strips on one side of the diamond, and a solid electrode on the opposite side. One applies an electric field, less than the breakdown field, across the thickness of the diamond. Under these circumstances the leakage current due to intrinsic carriers is extremely small (typically pA). A charged particle traversing the diamond creates electron-hole pairs (on average 36 pairs/micron traversed) which separate in the applied field. The motion of these charges induces a signal on the electrodes at the surface; the signal size being proportional to the distance the charges separate divided by the total thickness of the material [51]. At present, the distance the electron hole pairs move apart, the collection distance, is less than the typical thickness of the material. The collection distance of the diamond used in the first strip detector discussed below was $\sim 50\mu$m [52].

4.2 Recent Results

The practical use of diamond as a detector material [29] has been made possible by recent advances in the CVD growth process. This process allows diamond to be produced economically over a large area and with high purity relative to natural IIa diamond. During the last two years we have concentrated our efforts on the use of CVD diamond as a charge collection material in a diamond/tungsten sampling calorimeter [34] and as the active material in a 1 cm $\times$ 1 cm diamond strip detector [52].

As stated earlier and shown in fig. 4 the success of diamond devices was made

possible by the dramatic improvement in diamond quality which we attained by working closely with manufacturers. On the basis of our past experience and close working relations with manufacturers we anticipate continuing advances in this area.

Recently, in producing a diamond/tungsten calorimeter we were able to demonstrate that the CVD process can routinely produce large areas (360 cm^2) of high quality diamond. In this device the diamond is the active medium, the tungsten is the radiator. For comparison an identical silicon/tungsten calorimeter was constructed.

The calorimeter consisted of twenty layers of 3.0×3.0 cm^2 wafers of CVD diamond with an average thickness of 500 μm interspersed with 1 X_0 tungsten. The average collection distance of the diamond used in this device was 44 μm. The energy response and resolution (σ_E/E) were measured in 0.5 to 5.0 GeV electron beams at KEK and compared with the results from a silicon based calorimeter of identical construction. The results are [34]:

$$\frac{\sigma_E}{E} = \frac{(4.27 \pm 2.7)\%}{E} \oplus \frac{(19.13 \pm 0.86)\%}{\sqrt{E}} \oplus (2.3 \pm 1.8)\% \qquad \textit{Diamond} \quad (1)$$

$$\frac{\sigma_E}{E} = \frac{(3.89 \pm 0.87)\%}{E} \oplus \frac{(19.73 \pm 0.19)\%}{\sqrt{E}} \oplus (0.0 \pm 1.6)\% \qquad \textit{Silicon} \quad (2)$$

where E is given in GeV and $\oplus$ means added in quadrature.

The above results indicate that already diamond and silicon based calorimetric devices are comparable. The material used in this detector represents the first demonstration that a large amount of high quality CVD diamond can be produced and operated successfully.

Recently, we reached our minimum quality for fabricating tracking detectors where one charged particle must be detected. For this first test of a diamond strip detector we chose to construct a device with 100μm pitch and 50 μm strip width as shown in fig. 7. Initial source tests showed that with a strip pattern covering 50% of the active area there is no loss of charge relative to 100% coverage. The overall design of the detector is shown in fig. 8. The strip detector was constructed on an 8 mm $\times$ 8 mm $\times$ 300 μm diamond [53]. The 64 strips were 6.4 mm long. A guard ring was provided to keep edge leakage currents out of the active tracking volume and a shorting bar was used to gang strips into a single readout channel for initial testing.

A metallic Cr/Au contact was made to each side of the detector [32]. After coating each side of the diamond the strip pattern shown in fig. 8 was created using a wet etch process. Generally, the first metal in contact with the diamond determines the electrical properties of the contact. Chromium, titanium and other transition metals that form carbides tend to produce ohmic contacts to diamond. A current-voltage curve from a gang of six strips is shown in fig. 9 indicating very low levels of leakage current at full operation. In fig. 10 we show the collection distance for this sample. At approximately 100-125 Volts the slope of the collection distance changes as does the slope of the IV curve indicating a saturation of the carrier mobility, an increase in the number of carriers, and a change in the resistivity of the material. Such effects are common in diamond. For the material used in the tracking detector, below 200 V these effects do not influence the detector performance.

In fig. 11 we show a block diagram of the connections between the strip detector and external electronics. In this design, each strip was DC coupled (wire bonded) to an individual Viking preamplifier channel [54]. The detector bias voltage was applied to the common electrode and filtered locally. A test input was provided with a 5:1 divider to facilitate the pulsing of the entire device from the common electrode. In addition, a standard 1.8 pF capacitor was bonded to a preamplifier channel in order to test and calibrate the electronics.

In general the noise associated with the detectors should be small compared to that produced in the electronics. The noise contribution from the detector originates from three sources [54] (1) shot noise due to the statistical fluctuations in the leakage current; (2) bias resistor noise and (3) trace resistance noise. In diamond the first term is expected to be small since the leakage current is small. In our strip detector the leakage current was measured at the operating voltage to be less than 1 nA for the whole detector. For a typical peaking time of 2 μsec, a 1 nA leakage current produces 160 electrons noise. Assuming that this is shared uniformly among the 64 strips the contribution from leakage current to the single channel noise should be less than 20 electrons. The small leakage currents allowed the diamond detector to be DC coupled to the preamplifiers. In our case the bias resistor was effectively the feedback resistor of the preamplifier. In the normal running condition this resistor was more than 100 MΩ and hence it contributed less than 70 electrons to the noise. Finally the third source of noise depends on the strip resistance. In our detector the strip resistance was measured to be $\sim$ 15 Ω which is about $\frac{1}{15}$ of the equivalent channel resistance of the input FET in the preamplifier. Again this noise contribution can be neglected.

The position resolution measurement of the diamond detector was performed in a 50 GeV pion testbeam at CERN, using a telescope of eight silicon strip reference detectors. The reference detectors were single–sided, AC–coupled, 3×6 cm^2 silicon detectors with an implant/readout pitch of 25/50μm, equipped with microplex [55] electronics. They were arranged in 4 X–Y pairs, and each pair was connected to one readout processor (VME - SIROCCO) [56]. The precision of the individual reference detectors was about 6.5μm, which resulted in an extrapolation error of 3.5μm. This was more than adequate for the resolution we expected to achieve with the first diamond detector. All detectors were mechanically mounted on a granite/steel optical bench with an intrinsic precision of better than 1 mm. A trigger was provided by a pair of 1×1 cm^2 scintillators.

Data were taken only with normally incident beam particles. To analyze the data a standard charge-cluster search in the silicon reference counters for hits from beam particles [57] was performed. The search for charge-clusters in the diamond detector was performed as part of the final alignment procedure, using the same method with parameters appropriate for diamond. Figure 12 shows a typical plot of the Landau shaped cluster-charge in diamond and the distribution of mean values of the single channel noise of all strips, measured at $V_{bias} = 150$ V. This plot shows that the signal peak and the average measured noise level were separated by a factor of 6. The cluster search parameters have been optimised for each data sample. The average number of clusters per event found with these cuts was 1.4, and the average number of strips per cluster about 2.

Figure 13 shows the S/N distribution measured at $V_{bias} = 195$ V for the clusters

which were well matched to reconstructed tracks in the telescope. The data are fit with an approximation to a Landau distribution, and the most probable value found in this way was S/N = 6.3±0.2. Including a systematic uncertainty of ±0.50 (units of S/N) the S/N at V_{bias} = 195 V is equivalent to a most probable charge for a minimum ionizing particle of 875 ± 105 electron-hole pairs.

The residual plot in fig. 14 shows the hit precision of the diamond detector measured at V_{bias} = 195 V. The distribution was fit with a Gaussian which had a σ of 25.4 ± 0.9μm after correcting for the telescope extrapolation uncertainty. With the 6:1 signal to noise attained these results show a 12% improvement with respect to the digital hit precision which would be $100/\sqrt{12} = 28.9\mu$m.

The efficiency of the diamond was determined by comparing the number of tracks in the telescope and the number of clusters found in the diamond inside a window on the active surface of the diamond strip detector. The efficiency was determined as a function of the different cluster cut parameters. It showed only small variations around the parameters used for the cluster search. The optimal value found, for the data sample with V_{bias} = 195 V, was 86%. This represents a lower limit on the efficiency since dead readout channels and detector strips were not removed from the analysis.

4.3 Future Plans and Milestones

The results presented above indicate the feasibility of using diamond as the detection medium in a strip tracker. Achieving a signal-to-noise ratio of 6 : 1 and a position resolution of 25μm allows us to plan an improvement program in a number of areas to make these detectors a viable alternative to silicon for future high energy physics experiments.

One main area of research for the next three years consists of working with manufacturers to improve the quality of the diamond material. As stated in Sec. 2 methods have already been developed to increase the charge collection distance to 100 μm corresponding to a most probable signal of 2400 electrons. This is our milestone for the first year of the program. With this material we will demonstrate single and double sided detectors and measure their position resolution and efficiency in CERN test beams. We will also increase the size of the detectors from 1 cm × 1 cm to many cm^2. Of particular interest is a study of the strip width to pitch to optimize these devices. The optimum solution in diamond may not be the same as in silicon. For operation at the LHC preamplifier shaping times much shorter than those used here (50 ns compared to 2μs) must be envisaged. This will result in a baseline noise level of 600 to 700 e− in the electronics. We will continue to improve the diamond material in the second and third years in order to maximize the signal produced by the traversal of a minimum ionizing charged particle. To be a viable alternative for tracking we hope to operate at a signal-to-noise ratio of $\geq$ 15:1 with fast electronics.

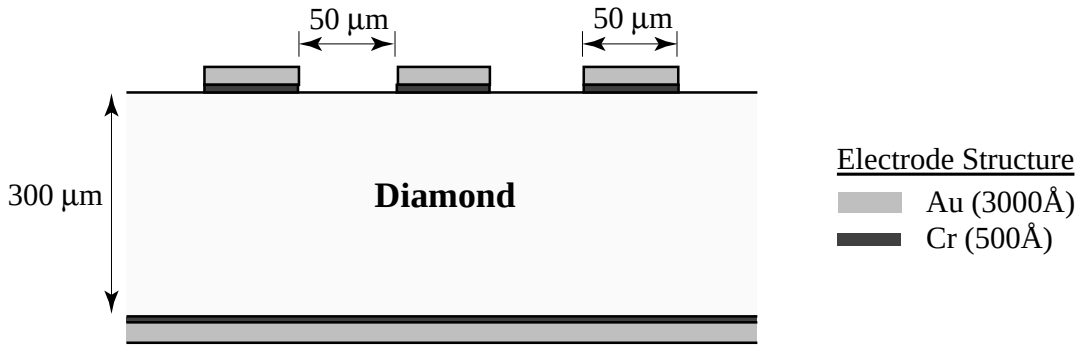

Figure 7: Cross section view of the diamond strip detector.

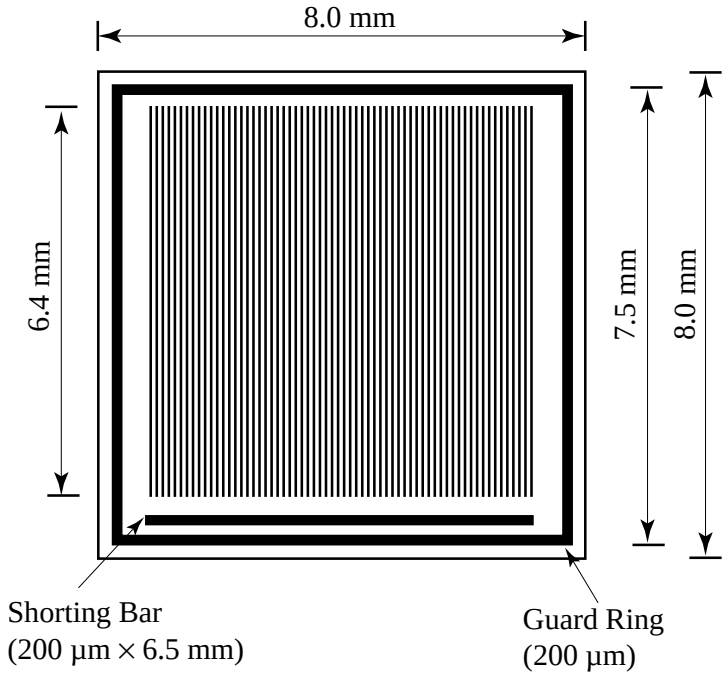

Figure 8: Schematic view of the diamond strip detector.

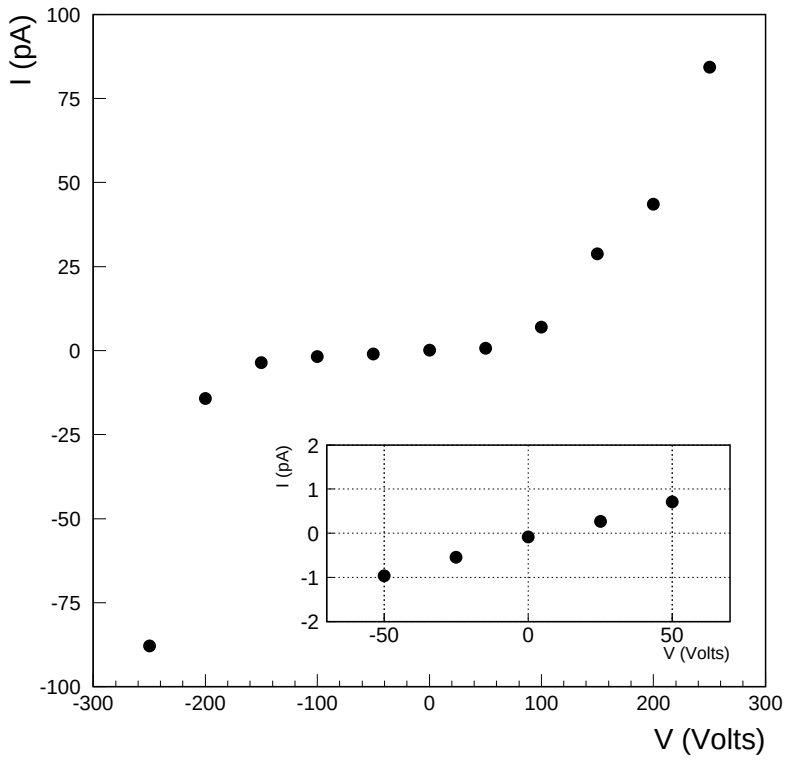

Figure 9: $I - V$ characteristics of six ganged strips from the diamond strip detector.

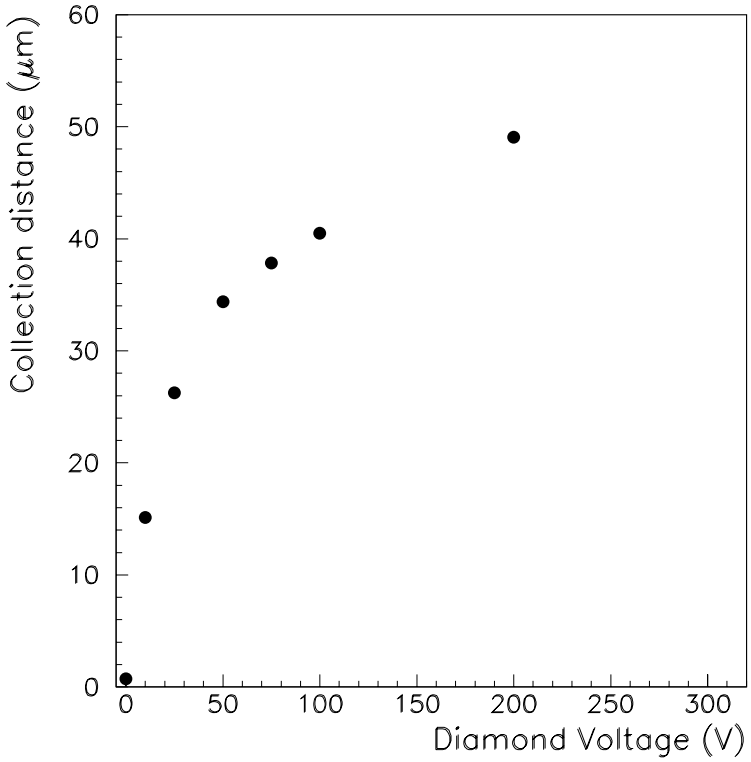

Figure 10: Charge collection distance as a function of bias voltage placed across the diamond.

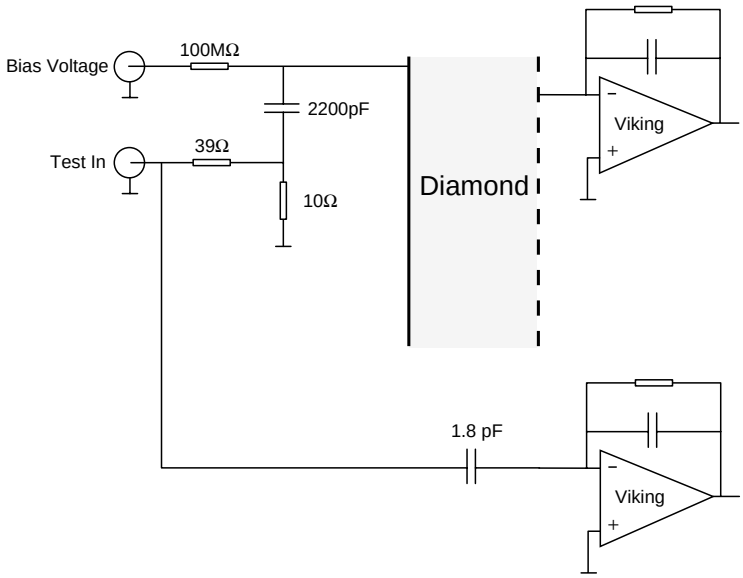

Figure 11: Block diagram of the support electronics for the diamond strip detector.

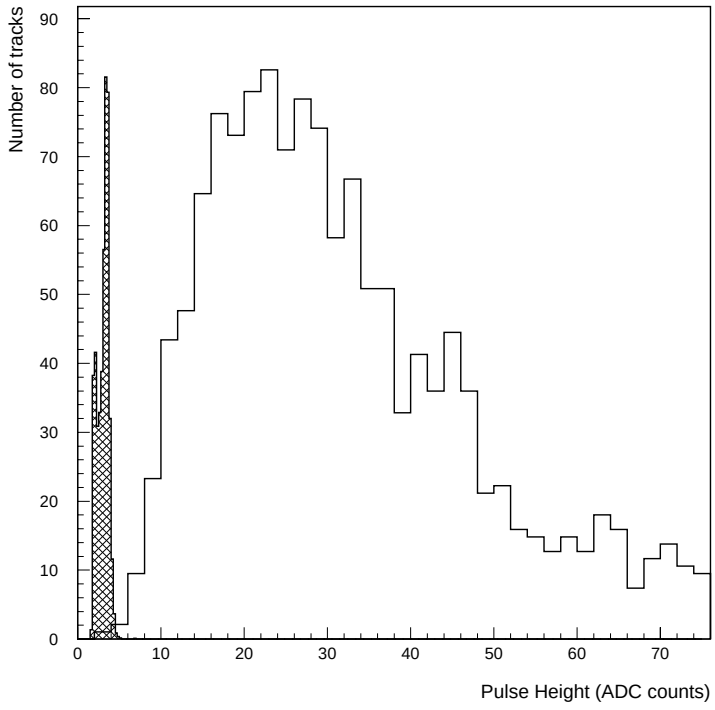

Figure 12: The raw signal distribution with the pedestal width (hatched) overlaid for comparison.

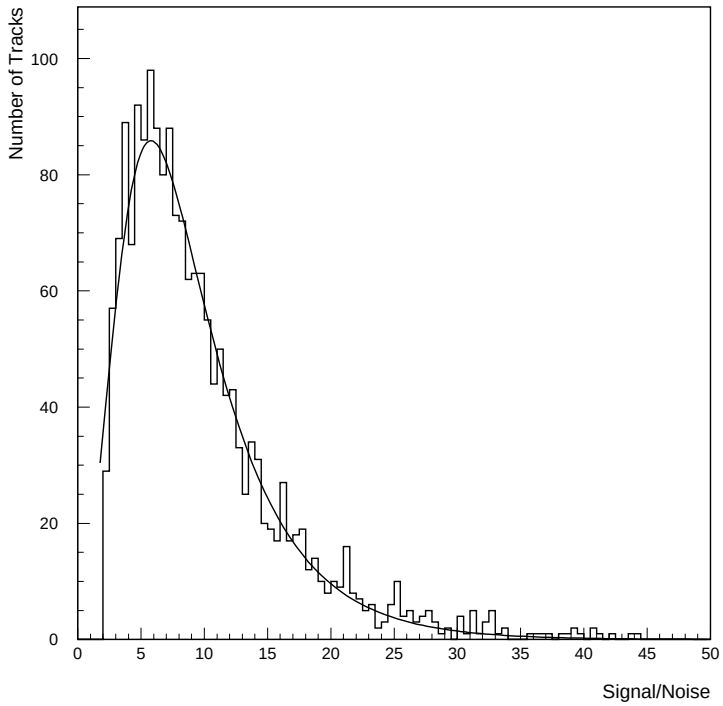

Figure 13: Signal-to-Noise distribution for hits which are well matched to charged particle tracks as predicted by the silicon telescope. The most probable signal is 6.3 ± 0.2 times the average single strip noise (N).

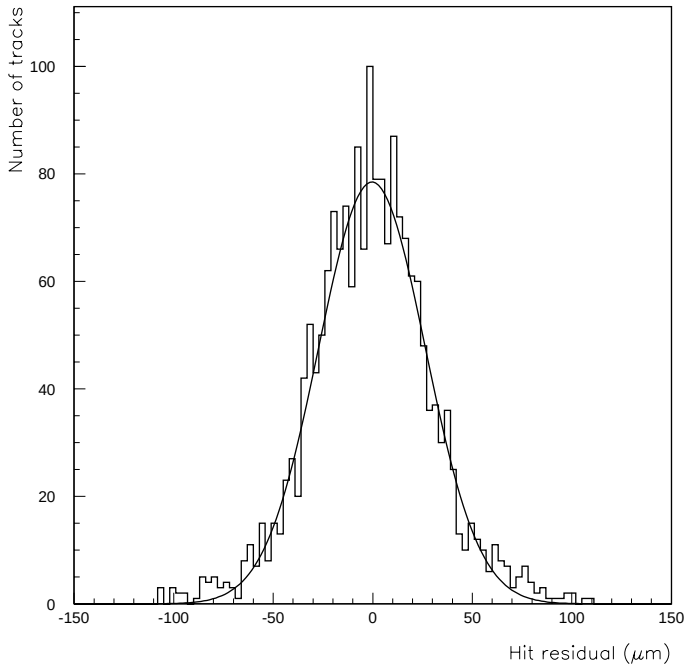

Figure 14: The experimental position resolution of the diamond detector, compared to the predicted charged particle impact point based on the silicon telescope information. The standard deviation of the single Gaussian fit is 25.4 μm.

5 Readout Electronics

The requirements for the front-end electronics for diamond detectors will be similar to those for silicon readout but more demanding both with respect to noise performance and radiation resistance. Since one does not expect to obtain signals with diamond detectors much more than one third of those obtained from a 300 μm thick silicon detector, the requirements on the noise performance for diamond readout electronics are a true challenge. This difficulty is, however, compensated for by the advantage that all detector noise sources, in the case of diamond, will very likely be negligible as stated above. Shot noise from leakage currents (expected to be in the pA range per strip), bias resistor noise and noise from the trace resistance are believed to be below 100-200 electrons ENC, even at the end of a full 10 years of high luminosity LHC running. The main noise sources for diamond readout will be the amplifier noise itself: the two main contributions will come from the series noise of the input transistor and from 1/f noise. The series noise can be reduced to the required low level by designing for high enough transconductance, which may imply an increased power consumption. The 1/f noise will depend on the chosen technology and processing parameters. A potential advantage in the use of diamonds is the high speed of signal collection which may be exploited by the electronics design.

There may, however, exist other fields where diamond detectors can find a unique application, with less demanding requirements on speed and radiation hardness. In such cases, electronics can be specially designed for very low noise performance to compensate for the relatively small signal expected from the diamond detectors. Consequently, the use of diamond detectors in high energy physics experiments and also possible industrial applications can already be realistically envisaged. In all cases it will be possible to profit from substantial developments in this field which have been achieved for low noise silicon detector readout at the LHC [54, 58, 59, 60, 61, 62].

In the following, the necessary development or adaptation of suitable front-ends for both cases will be outlined.

5.1 Front-End Electronics for Diamond Detectors at the LHC

The best radiation-hard diamond detectors, which may be available in a few years, could have charge carrier lifetimes equivalent to an "available" charge of around 7000 electron hole pairs. Though this may seem a very small charge compared to what can be obtained with silicon detectors, it can be sufficient to construct a well-performing detector system. In silicon detectors one has to foresee deterioration in charge collection efficiency, substantial increase in leakage current, interstrip capacitance and intolerably high values of depletion voltage for equivalent doses in excess of several times 10^{14} n/cm^2. One can expect that diamonds do not change their characteristics after similar radiation doses. In this case, one can accept a lower S/N ratio compared with silicon at the beginning of the experiment. The challenge will be to develop electronics radiation hard enough to perform with little deterioration up to the highest radiation doses. Existing radiation hard processes [†] have been tested up to a level of

[†]For example the AVLSIRA bulk CMOS process from Harris or the SOI technology available at Thomson in Grenoble.

about 100 kGy with little deterioration of noise performance [63, 64].

The JFET-CMOS technology [‡] also shows promise. It exploits the intrinsic low noise and radiation hardness properties of the JFET. CMOS devices are realised in a SIMOX technique, and bringing along a considerable increase in speed with respect to bulk implementation. Front-end circuits based on this technology have been proven to stand high gamma ray doses [65], without degrading their noise performance at shaping times below 100 ns (see fig. 15a and b). Therefore, the JFET-CMOS-SIMOX process is a viable solution for circuit design aiming at complying with the requirements of experiments at high luminosity colliders. As a first step, a charge-sensitive preamplifier with a continuous time charge restoration was realised and showed a very good noise behaviour (ENC = 600 e^- at 100 ns signal peaking time, with a 7 pF detector capacitance and 2.5 mW power consumption – see fig. 16). The circuit architecture tested in this preamplifier prototype has been used in the design of a 32 channel front-end system. Each channel consists of a charge sensitive preamplifier and a continuous time filter, implementing a unipolar signal shaping with 50 ns total duration. The system is tailored to detector capacitances of 5 to 15 pF.

Existing readout architectures, as developed for LHC experiments as front-ends for silicon detectors (for example the RD20 deconvolution front-end), will be a starting point for such developments. Adaptation of the input FET to the expected low load capacitances will yield a pre-amplifier shaper circuit with the following noise characteristics: ENC = 300 e^- + 50 e^-/pF after deconvolution.

For 12 cm long strips at 50 μm pitch, one can expect a total load capacitance of about 5 pF. This would lead to a series noise of about 600 electrons and a signal to noise of 10 to 12 for time stamping and of about 18 for the undeconvoluted peak pulse height (assuming 7000 charges for a minimum ionising particle). The possibility that the detector leakage current will be negligible even after very high radiation doses, makes the RD20 slow/fast filtering scheme [60] very attractive, since the relatively low noise amplitude from slow shaping can be used throughout the lifetime of the experiment for precise coordinate calculation. Under such circumstances, a deterioration of the front-end noise performance of about 50% could possibly be tolerated. Also the very fast charge collection time (less than 1 ns) in diamond may be an important factor in an optimal exploitation of the deconvolution scheme.

Similar noise figures have recently been obtained with a very fast bi-polar preamplifier/shaper developed in RD20 for the ALICE experiment for silicon drift detector readout. This amplifier has a risetime of 15ns and would thereby make optimal use of the signal speed in diamond. Adaptation to the diamond detector properties and further development to achieve lowest possible noise of this circuit will be an important part of our research program.

5.2 Very Low Noise Front-Ends for Other Applications

In the early stages of this programme, it is expected that diamond material will improve slowly. Carrier lifetimes in the order of 1 to 10 ns may be achieved,

[‡]Available from the Fraunhofer Institute for Microelectronics Circuits and systems in Duisburg, Germany.

corresponding to less than one thousand and up to a few thousand charges seen by the amplifier.

The emphasis in the readout electronics will be directed towards very low noise and relatively slow charge sensitive amplifiers. While limitation in power consumption is always desirable, it is at this stage not an important constraint.

A promising line will be further improvement and adaptation of the Viking amplifier to specific diamond detector properties. Given the low dielectric constant (in comparison with silicon) of diamond and strip pitches on the order of 50-100 μm, one expects detectors capacitances in the order of 0.3 to 0.5 pF/cm, including backplane capacitance. This implies that a sensor of useful size may have a total load capacitance of one strip on the order of 2-3 pF.

The Viking concept, which was designed for LEP applications, has been optimised so far for capacitance loads of 15 to 25 pF. The Viking amplifier originally developed as a 12 channel prototype chip (in 1.5 μm MIETEC technology), consisting of a preamplifier, shaper, and sample and hold. The circuit is based on a folded cascode configuration with a very low noise input FET. The feedback is obtained by a resistor with very high effective resistance (more than 100 MΩ) and a feedback capacitor of about 0.4 pF. The shaping circuit is basically a replica of the pre-amplifier stage.

The noise performance has been measured to be ENC = 135 e^- + 15 e^-/pF [62] for a CR-RC shaping with a pulse peaking time of about 1.5 μs.

Several improvements to this circuit have meanwhile been implemented. A 128 channel version has been designed, tested and is already in wide spread use. This chip has a shift register at the output to read out sequentially all 128 channels upon an external trigger. Each individual input can also be addressed via a shift register, which connects a test input capacitance to the selected channels.

An improved circuit designed for high (roughly 60 pF) input capacitances has been implemented in 1.2 μm AMS technology and tested. The noise performance is significantly better than in the previous Vikings. With an input FET capacitance of about 10-12 pF, the noise has been measured to be 200 e^- + 6 e^-/pF at 2 μs shaping time.

Results achieved with these circuits allow us to predict the performance of a readout chip tailored to the readout of diamond strip detectors. Choosing the input FET to have about 500 μm width, one can expect to achieve a transconductance of g_m= 5 mA/V, leading to a noise slope of 10 e^-/pF at a shaping time of 1 μs. The effective input capacitance of the preamplifier of 1-2 pF should result in ENC = 40 e^- noise for an unbonded channel. This would lead to a serial noise of 100 e^- for a 6 cm long strip, if one can limit parallel noise from "leakage" current and feedback resistor and serial noise from the metal strips of the detector to less than 20 e^- ENC. To achieve this, the feedback resistor has to be higher than 2 GΩ, the leakage current less than 100 pA per strip, and the resistance of the metallisation less than 20 Ω for the entire length of the strip. With presently existing diamond material, S/N ratios in the order of 12 to 14 could be reached.

Figure 15: Effect of ^{60}Co gamma rays on the noise behaviour of a JFET-CMOS-SIMOX preamplifier. a) series noise voltage spectrum; b) equivalent noise charge at C_D = 10 pF. The preamplifier was followed by a bipolar $(CR)^2 - (RC)^2$ shaper.

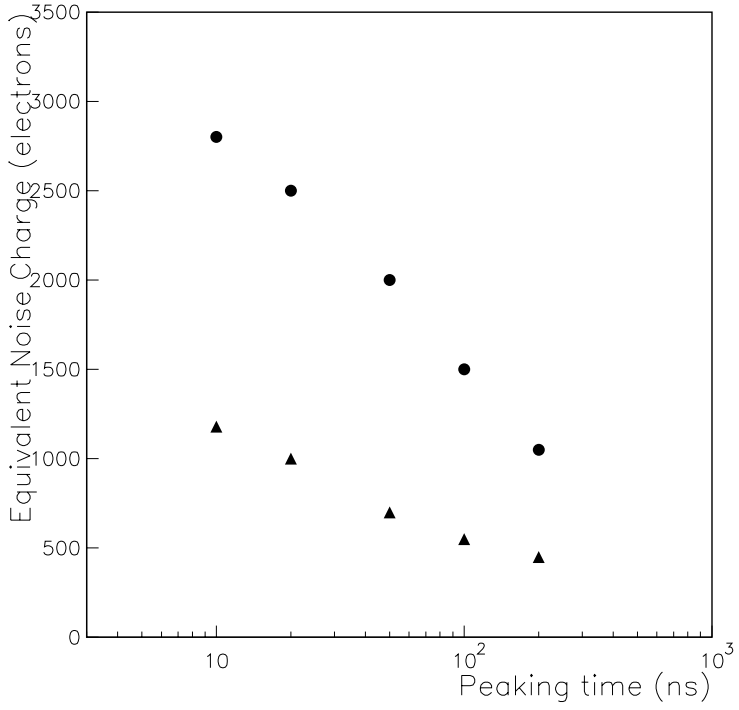

Figure 16: Equivalent noise charge as a function of the signal peaking time for a fast charge sensitive preamplifier in JFET CMOS technology. The preamplifier was followed by an RC-CR shaping amplifier. Circles (triangles) are measurements made with a load capacitance of 17 (7) pF.

6 Other Applications of Diamond

In addition to its potential use as a detector material, with radiation hardness possibly superior to that of silicon, diamond is of considerable interest due its unique combination of mechanical properties - those of lightness (ρ = 3.5 g cm^{-3}) and extremely high thermal conductivity (in the range 1000 - 2000 W m^{-1}K^{-1}; up to five times greater than that of copper at room temperature).

6.1 Thermal Management

The thermal management of the large, high precision solid state central tracking and vertexing detectors proposed in future hadron collider experiments, for example in the ATLAS and CMS detectors at the LHC, will require the efficient removal of heat generated by the sophisticated high speed readout electronics of several million strip detector channels and up to 50 million individual pixel detector electronic readout cells [66]. In addition to the heat generated in the readout electronics, the silicon detectors themselves also exhibit a gradual increase in heat dissipation over their entire area as their leakage current increases under exposure to the very high radiation levels expected at LHC [12].

A number of groups involved in solid state tracking detector R&D for LHC detectors are studying their thermal management [6]. Both convective and conductive heat evacuation techniques are under evaluation.

Direct convective cooling by flushing the detector volume with cold gas has several attractive features - in particular, the minimal amount of extra material presented by the cooling system. However, the comparatively low heat capacity of the gas suggests that while the technique might be viable for the removal of the lower levels of uniformly - distributed leakage current - related heat in irradiated silicon detectors, it will probably be unable to remove the much greater heat dissipated locally by the readout electronics.

Conductive cooling schemes direct heat to be evacuated into fluid circulating in closed channels directed as close as possible to the sources of maximum dissipation. In a single phase coolant configuration - which could be a flow of water with ethylene glycol or alcohol, or of a fluorocarbon liquid, for example from the 3M fluorinent range - the fluid mass flow is chosen in accordance with its heat capacity and the amount of heat to be removed. Circulation of a bi-phase cooling fluid can in principle allow greater heat absorption - making use of the latent heat of vaporization in the case of a liquid - gas phase change (ammonia and fluorinent fluids are currently under investigation) - or the heat of fusion in the gas of a solid - liquid transition (for example in the case of a "binary ice" suspension of microscopic ice crystals in water and ethylene glycol). While the ultimate efficacity of any conductive cooling scheme also depends on the series thermal impedance between the heat sources and the coolant fluid channels, the physics requirement of minimal multiple scattering demands very low mass structures which preclude the traditional use of a substantial thickness of metal for heat sinking.

6.2 A Specific Example

Figure 17 is an example, at the full detector layer level, of a possible low mass support structure designed to evacuate the heat dissipated in pixel detector readout electronics into axial liquid coolant channels. In this example, pairs of silicon pixel detector wafers - each 60 x 20 mm^2 and carrying readout electronics which dissipates around 0.2 - 0.4 W cm^{-2} over their entire area - are attached together and to the support cylinder by pairs of low mass heat sinks. The paired detector wafer arrangement is of interest since it halves the number of axial fluid cooling channels - which would present a serious material shadow at low radius.

The support structure of figure 17 has an inner "shark's tooth" profile to provides flat mechanical and thermal attachment points for the heat sinks, and to give the detectors an overlap in azimuth.

Thermal studies of heat sinking in this geometry using miniature heat pipes (cross section 2.5 x 8 mm^2) have given quite promising results [67], with temperature variations less than 5 °C over detector wafers in the geometry of fig 17. While low mass heat pipes (with very thin wall aluminum extruded envelopes) would probably satisfy the low mass/high conductivity requirement (and are still under investigation), there is concern about their long term reliability under irradiation at the high levels expected at LHC, which might cause the formation of non- condensible gas that would impede the phase change on which their high conductivity depends: a light, radiation hard, solid state heat sink material is clearly an attractive alternative.

6.3 The CVD Diamond Solution

In recent years, CVD diamond films have become widely used as heat spreaders in very high power density applications such laser diode heat sinking and multichip module packaging [68, 69, 70], both of which are much more thermally demanding applications than our own. Diamond substrate material is available off the shelf from several manufacturers with thicknesses up to 500 μm, and in areas as large as several times 10 cm^2. It is already possible to order CVD diamond in the same geometry as the miniature heat pipes in the geometry example of fig. 17. The coefficient of thermal expansion of CVD diamond is better matched to that of silicon than most other commonly used hybrid substrate materials (see table 4). Other possible cooling geometries, including the hybridization of readout electronics on diamond substrates and the lamination of diamond heat spreaders onto large area silicon detector base modules are being considered.

CVD diamond film is very attractive in our solid state tracker application for its low mass, robustness and high thermal conductivity. We plan to investigate its suitability as a heat sink to conduct the significant heat dissipated by the detector readout electronics into a circulated coolant.

Diamond substrate material is already available in a geometry which allows the direct replacement of miniature heat pipes in one geometry that is already under study: one of our first investigations of CVD diamond will naturally be in this application. We plan to make comparative studies of heat dissipation from electronics mounted on diamond and other common insulating hybrid substrate materials, in-

Material	Thermal Conductivity (W/m/K)	Thermal Expansivity (10^{-6}/K)
CVD Diamond	1000 -2000	0.8 - 1.2
Silicon	150	2.6
GaAs	45	6.9
Alumina (99%Al_2O_3)	29	6.5
Aluminium Nitride (AlN)	70 - 230	3.3
Beryllia (BeO)	223	6.4
Copper	396	17.0
Silver	428	19.0

Table 4: Thermal properties of various materials commonly used in solid state trackers.

cluding beryllia, aluminium nitride and alumina. We also plan to study the cooling of readout electronics on diamond substrates and lamination of diamond heat spreaders onto silicon large area detector base modules.

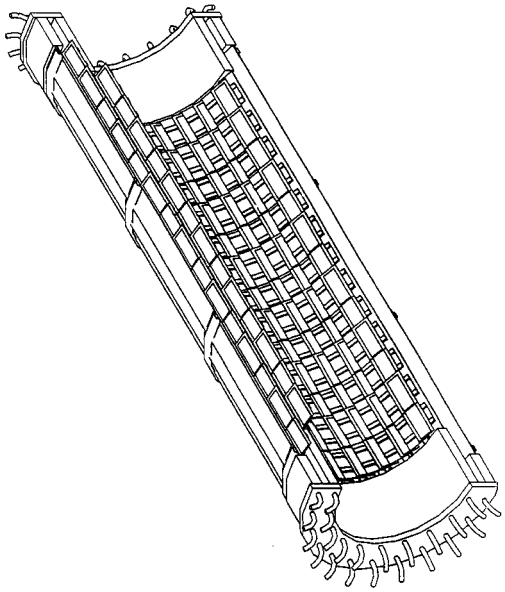

Figure 17: A possible cooling and support structure for a pixel detector at the LHC (radii 11.5 and 14 cm and having a length of 80 cm).

7 Summary of Proposed Research

The possibility of extending LHC tracking detector's reach to smaller radii and greater rapidities is quite exciting. Our proposal is aimed at studying if diamond's extraordinary physical properties will allow us to build detector components which can survive in the harsh LHC radiation environment and still make the precision track measurements necessary to explore the physics outlined in section 1.

Our main area of research for the next three years will be to work with manufacturers to improve the quality of the diamond material. Methods have already been developed to increase the charge collection distance to 100 μm corresponding to signal of the order of 2400 electrons. This is our milestone for the first year of the program. With this material we will produce single and double sided strip detectors and measure their position resolution and efficiency in CERN test beams. We will also increase the size of the detectors from 1 cm $\times$ 1 cm to many cm^2. Of particular interest is a study of the ratio of the strip width to pitch to optimize these devices. The optimum solution in diamond may not be the same as in silicon.

The growth of high quality CVD diamond for particle detectors can be achieved with a strong laboratory, university and industrial effort. Because of the large number of variables during the growth process systematic correlations between growth parameters and film quality must be extended. Our collaboration has the expertise to quantify the results of the growth process. We intend to use this expertise to provide rapid feedback to diamond manufacturers on the quality of their products thereby continuing the rapid increase in electrical properties we have recently attained.

In order to test the radiation hardness of the material produced we plan to expose samples of the newest CVD diamond material to neutron, alpha and ^{60}Co sources as new generations of the material become available. We also expect to establish a study of irradiation with protons and charged pions. To improve the understanding of the mechanisms at work in irradiated CVD diamond we also propose to investigate quantitatively the production of specific defects (vacancies, interstitials and their complexes), by irradiation, to see which defects affect the electronic properties. From these studies we expect to demonstrate whether variations in the production process affect radiation hardness and to work to optimise the growth of radiation-hard diamond.

In the first year of our program we plan to produce a low noise VLSI tracker readout chip whose working point is optimised for the low capacitance loads typical of diamond trackers. We will begin to study the implementation of such chips in a radiation hard process (such as the Harris technology). In later years we will concentrate on approaching the readout speeds necessary for the LHC (while maintaining sufficiently low noise to readout diamond signal) and attaining the radiation hardness necessary for the electronics to survive in the LHC environment.

During the second and third years of our program we will continue to improve the diamond material and develop more sophisticated detectors ultimately reaching our long term goal of 7000 electrons most probable signal for traversal of a minimum ionizing charged particle and 15:1 signal to noise with electronics appropriate for the LHC.

8 Manpower, Infrastructure and Funding

What follows is a breakdown of the areas of research that will be pursued at the different institutes (table 5) involved in the project, a budget for the work to be carried out (table 6) and sources of funding expected for the project (table 7).

8.1 Requests from CERN Infrastructure

It is anticipated that in addition to funding to purchase diamond samples and develop radiation hard low noise electronics that the following requests will be made on the CERN infra-structure:

- four 5-day testbeam running periods per year for the duration of the project;
- computing time and disk space on the central CERN computers (see separate COCOTIME application);
- 30 m^2 of laboratory space for test setups, detector preparation and electronics development;
- office space for 3 full time residents and 10 visiting members of our collaboration;
- access to CERN stores.

Institute	1	2	3	4	5	6	7	8	9	10	11	12	13	14
Diamond Characterisation	x	x			x	x	x		x		x			
Radiation Hardness	x			x	x	x	x		x	x			x	
Detector Design			x	x	x				x		x		x	x
Low Noise Electronics		x	x					x				x		x
Rad.Hard Electronics			x					x			x	x		
Heat Sinks/Electronic Substrates				x						x				
Data Analysis		x			x			x					x	x

Table 5: Research Interests of groups involved (1=Aveiro, 2=Bristol, 3=CERN, 4=CPPM, 5=Imperial College, 6=King's College, 7=LLNL, 8=LEPSI, 9=LANL, 10=MPI-Heidelberg, 11=OSU, 12=Pavia, 13= Rutgers, 14=Vienna).

Item Budget	(Year 1)	(Year 2)
Raw Diamond Material and Characterisation	245	430
Detector Fabrication	30	50
Low Noise Electronics	80	40
Radiation Hard Electronics	40	120
Thermal Grade Diamond	30	40
Auxiliary Electronics	60	60
Offline Computing	30	30
Travel	60	80
Totals	575	850

Table 6: Estimated Budget (in kCHF).

Institute (Anticipated Funding)	(Year 1)	(Year 2)
Aveiro	20	20
U.K. (HEP)	100	100
U.K. (non-HEP)	20	20
CERN	180	180
CPPM	20	20
LEPSI	25	50
Milan/Pavia	20	20
MPI-Heidelberg	20	20
U.S.A. (LLNL,LANL,OSU,Rutgers)	150	400
Vienna	20	20
Totals	575	850

Table 7: Funds (in kCHF) subject to approval of national funding agencies.

References

[1] ATLAS Collaboration, LHCC 92-4, CERN; LHCC/I 2 (1992); LHCC 93/53, CERN.

[2] CMS Collaboration LHCC 92-3,CERN; LHCC/I 1 (1992) CERN; B Physics and CP Violation Studies in CMS, LHCC 93-49, CERN.

[3] COBEX Collaboration, LHCC 93-50, LHCC/I 6 CERN, LHCC 94-14, CERN.

[4] GAJET Collaboration, LHCC 93-54.

[5] LHB Collaboration, LHCC 93-45.

[6] "Development of High Resolution Silicon Strip Detectors for Experiments at High Luminosity at LHC RD20 Collaboration: Status Report to CERN DRDC"CERN/DRDC 93-30.

[7] A. Rudge, Investigation of fast amplifier with a diamond detector. Submitted to the Pisa meeting (May 1994).

[8] P. Choi, "Diamond in Plasma Physics Applications",Proceedings of Diamond Detector Workshop, Imperial College, 21-22 February 1994.

[9] CMS TN 92-59,"Delta Ray Effects in Silicon Strip Detectors", M. Huhtinen.

[10] FLUKA92, A. Fasso *et al.* Proc. Workshop on Simulating Accelerator Radiation Environments, Santa Fe, 11-15 Jan 1993. HERA-B Studies are based on FRITIOF, A. Abduzhamilov *et al.*, Z. Phys. **C40** (1988).

[11] CMS TN 93-77 "Radiation Hardness of the CMS Tracker", G. Hall, C. Hauviller, T. Meyer.

[12] "Radiation Doses Expected at LHC an update": T. Mouthuy: ATLAS INDET-NO-028.

[13] CMS TN/92-35, CMS TN 94-135 "Radiation Problems at LHC...", M. Huhtinen, P. Aarnio.

[14] HERA-B Progress Report, DESY-PRC 93/04, DESY.

[15] S. Gadomski, "B_s mixing in ATLAS", presented at Beauty '94, Mt.St.Michel, April 1994.

[16] See, for example, J. Hassard, S. Margetides, "Tracking for B Physics in CMS", Proc. Snowmass Meeting on B physics in Hadron Colliders, July 1993.

[17] CMS TN/92-48 "Search for charged Higgs boson with CMS detector at LHC".

[18] G. Ridolfi *et al.* Proc. LHC Workshop, Aachen, Vol II, ECFA 90-133, 1990 and references therein.

[19] Daniel Froidevaux "Top Quark Physics at LHC/SCC" (sic) CERN/PPE/93-148, 1993.

[20] Karl Gill, Ph.D. Thesis, Imperial College, 1993.

[21] CMS TN 93-85 "The 4 lepton Higgs Decay Channel...", C. Seez.

[22] CMS TN-123 This shows the advantages of jet tagging in very forward calorimeters.

[23] See CMS TN/93-122 "SUSY Higgs Searches at Future Colliders", G. Wrochna.

[24] CMS TN/93-103, "Search for the Heavy Neutral MSSM Higgs...", D. Denegri and R. Kinnunen.

[25] CMS TN/92-34 "Determination of the Top Quark Mass", A. Kharchilava.

[26] P. Eerola *et al.* "CP violation and B Physics in the ATLAS Detector"; TN 93-121 D. Denegri *et al.* "CP violation and B Physics in the CMS Detector", November 1993.

[27] I. Dunietz, CP Violation with Self-Tagging B_d modes, CERN TH-6161/91 (1991).

[28] CMS TN/92-33 "Physics with Heavy Ions in CMS Detector", M. Bedjidian *et al.*

[29] M. Franklin *et al.*, Nucl. Instr. and Meth. **A315** (1992) 39.

[30] J. Angus and C. Hyman, Science **241** (1988) 913; and W. Yarbrough and R. Messier, Science **247** (1990) 688.

[31] M.A. Plano *et al.*, Appl. Phys. Lett. **64** (1994) 193.

[32] S. Zhao, Ph.D. Thesis, The Ohio State University (1994).

[33] S. Zhao *et al.*, Mat. Res. Soc. Symp. **Vol 302** (1993) 257.

[34] R.J. Tesarek *et al.*, submitted to Nucl. Instr. and Meth.

[35] S. Dannefaer and D. Kerr (1992) Diamond Related Mater. **1** 407.

[36] G. Davies, S. C. Lawson, A. T. Collins, A. Mainwood and S. J. Sharp (1992) Phys. Rev **B46** 13157.

[37] D. W. Palmer in "Properties of Diamond—a DataReview" ed. G. Davies (IEE: London) (1994).

[38] J. N. Lomer and A. M. A. Wild (1971) Phil. Mag. **24** 273.

[39] for example A. T. Collins and P. M. Spear (1986) J. Phys. C **19** 6845.

[40] A. T. Collins (1977) Inst. Phys. Conf. Ser. **31** 346.

[41] L. S. Pan, D. R. Kania, P. Pianetta, J. W. Ager, M. I. Landstrass and S. Han (1993) J. Appl. Phys. **73** 2888.

[42] G. Davies, E. C. Lightowlers, R. C. Newman and A. S. Oates (1987) Semicond. Sci. Technol. **2** 524.

[43] E. R. Vance, H. J. Milledge and A. T. Collins (1972) J. Phys. D **5** L40.

[44] E. W. J. Mitchell in "Physical properties of diamond" ed R Berman (Clarendon: Oxford) (1965).

[45] L.S. Pan *et al.*, work in progress to be submitted to Appl. Phys. Lett.

[46] S.F. Kozlov *et al.*, "Preparation and Characteristics of Natural Diamond Nuclear Radiation Detectors", IEEE Transactions on Nuclear Science **NS-22**, 160 (1975).

[47] M. Geis, MIT Lincoln Laboratory, private communication.

[48] S.M. Sze, **Physics of Semiconductor Devices**, 2nd edition, John Wiley and Sons, New York (1981).

[49] J. Prins in "The properties of natural and synthetic diamond" ed. J. E. Field (Academic Press: London) (1992).

[50] R. Kalish in "Properties of Diamond—a DataReview" ed. G. Davies (IEE: London) (1994).

[51] L.S. Pan *et al.*, J. Appl. Phys. **74** (1993) 1086.

[52] F. Borchelt *et al.*, submitted to Nucl. Instr. and Meth. (1994).

[53] The CVD diamonds were provided by St. Gobain/Norton Diamond Films, Northboro Research Center, Goddard Road, Northboro, MA 01532.

[54] E. Nygård *et al.*, NIM **A301** (1991) 506.

[55] J. Stanton and N. Kurtz; RAL–89–028 Rutherford Appleton Laboratory.

[56] C. Colledani *et al.*, A High Resolution Beam Telescope, CRN-LEPSI note, to be published.

[57] R. Turchetta, Ph.D. Thesis, N. 1019, Strasbourg, France (1991).

[58] R. Brenner *et al.*, NIM **A330** (1994) 564.

[59] R. Brenner *et al.*, NIM **A339** (1994) 477.

[60] R. Bingefors *et al.*, NIM **A326** (1993) 112.

[61] S. Gadomski *et al.*, NIM **A320** (1992) 217.

[62] O. Toker *et al.*, NIM **A340** (1994) 572.

[63] M. Raymond, Harris Test Structure Noise Measurements, RD20/TN/25.

[64] W.Dabrowski and J.Kaplon, Noise Measurements of Harris Transistors, RD20/TN/30.

[65] G. Cesura *et al.*, NIM **A344** (1994) 166.

[66] ATLAS Collaboration Letter of Intent, CERN/LHCC/92-4 LHCC/I2: (October 1,1992)

[67] L. Patrone, "Transfert Thermique dans un Detecteur de Particules a Semiconducteur", (CPPM) (30/6/93) Rapport de Stage de Maitrise de Physique et Applications, Faculte des Sciences de Luminy.

[68] R.C. Eden, "Application of Synthetic Diamond Substrates for Thermal Management of High Performance Electronic Multichip Modules"; "Applications of Diamond Films and Related Materials": eds. Y; Tzeng, M. Yoshikawa, M. Murakawa and A. Feldman, (Elsevier Science Publications BV, Amsterdam 1991), 259.

[69] G. Lu *et al.*, "Free Standing White Diamond for Thermal and Optical Applications" Diamond and Related Materials 2 (1993), 1064 (Elsevier Sequoia).

[70] D. Norwood *et al.*, "Diamond - a new high Thermal Conductivity Substrate for Multichip Modules and Hybrid Circuits": Sandia National Laboratory, Dept 2411 Report 1993 Proc. 43rd Electronic Components and Technology Conference, June 1-3 1993